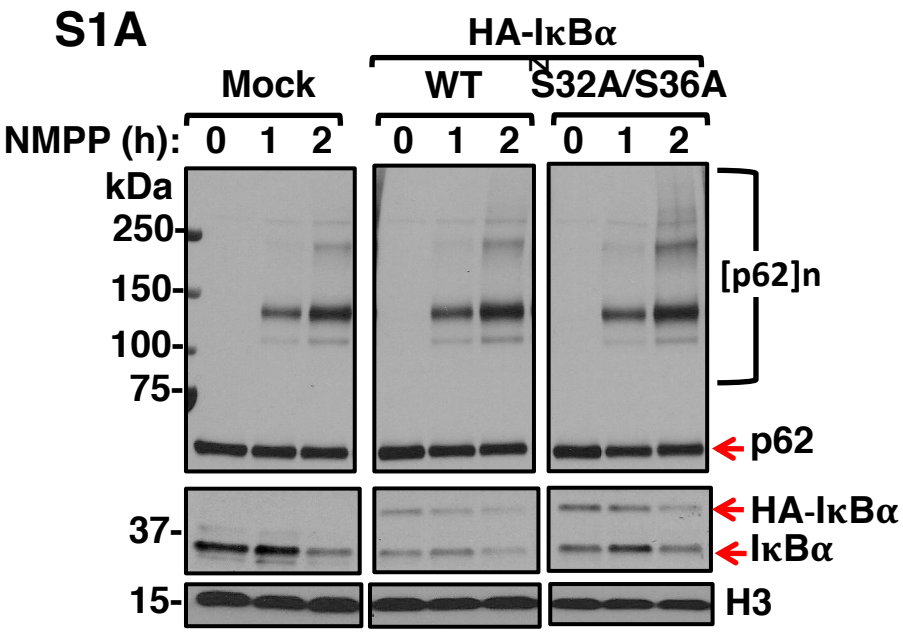

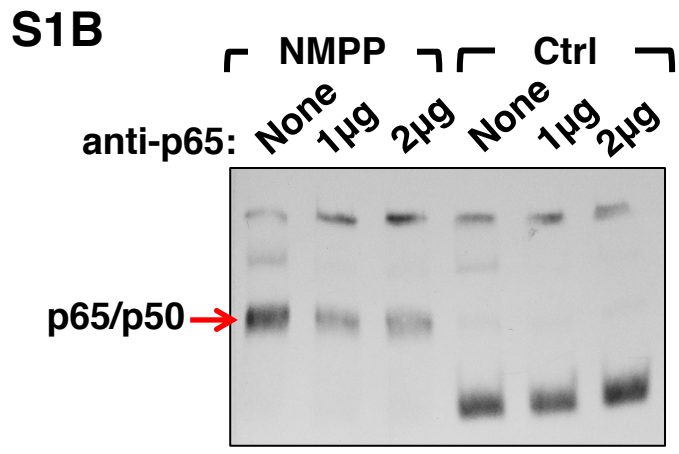

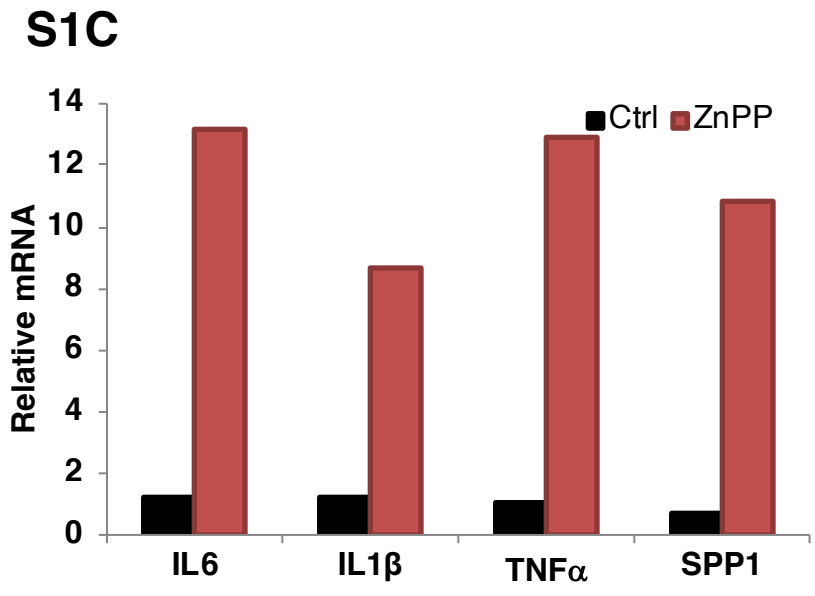

FIGURE S1. NMPP-elicited PPIX-accumulation with concurrent NFκB activation and IκBα-loss is independent of proteasomal degradation, PPIX and ZnPP are even more potent elicitors of IκBα-loss and p62-aggregation than NMPP (Related to Fig 1). **A**. HepG2 cells were transfected with pCMV4-3HA-IκBα or mutant pCMV4-3HA-IκBα-S32A/S36A for 40 h, then treated with NMPP for the indicated times. Cell lysates were subjected to IB analyses of p62 and IκBα with histone H3 as the loading control. **B**. Supershift EMSA using nuclear extracts from Fig 1C (4 h NMPP sample and No treatment (None) sample) with p65-antibody verifies the identity of the p65/p50 band. **C**. qRT-PCR analyses of mRNA from intact livers of mice injected i.p., daily with ZnPP (50 μmol/kg) or vehicle controls (Ctrl) for 7 d (Mean, n = 2). SPP1, osteopontin or secreted phosphoprotein 1.

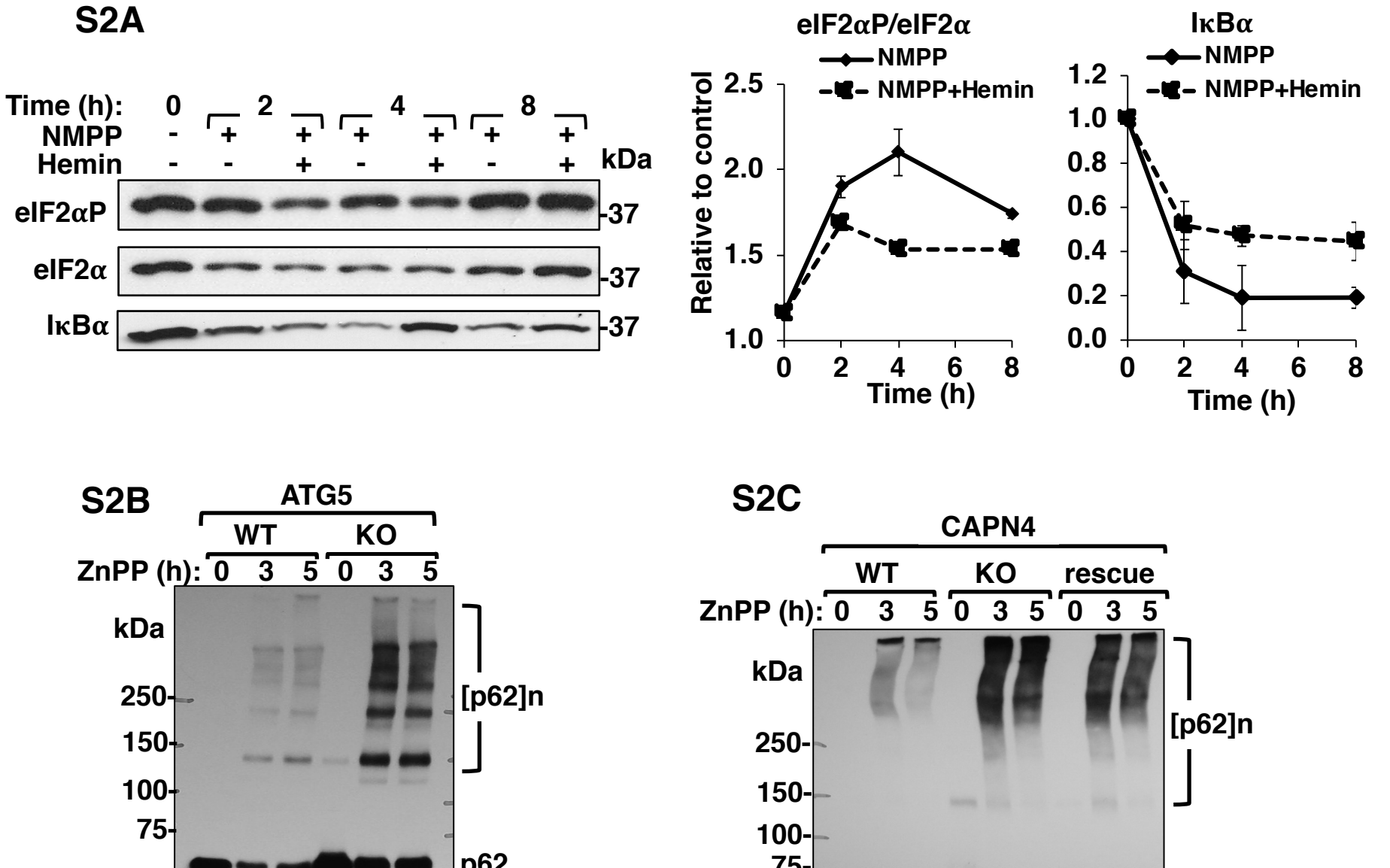

FIGURE S2. ZnPP-elicited IκBα-loss is independent of heme deficiency triggered HRI-activation, autophagy and calpain-mediated proteolysis (Related to Fig 1). **A**. IB analyses of eIF2α, eIF2αP and IκBα in lysates from mouse hepatocytes treated with NMPP or NMPP plus hemin for the indicated times. The temporal profiles of the ratio of eIF2αP to total eIF2α as well as IκBα content were determined (Mean ± SD, n = 3). **B**. ATG5 wild-type (ATG5WT) and knockout (ATG5KO) MEF cells were treated with ZnPP (10 μM) for the indicated times. Cell lysates were used for IB analyses of p62, IκBα, and LC3, with actin as the loading control. **C**. MEF cells wild-type calpain (capn4WT), capn4 knockout (capn4KO) and capn4KO-rescue (wherein capn4 knockout cells were rescued by transfection of a Capn4 lentiviral vector) were treated with ZnPP for the indicated times. Cell lysates were used for IB analyses of p62 and IκBα with actin as the loading control.

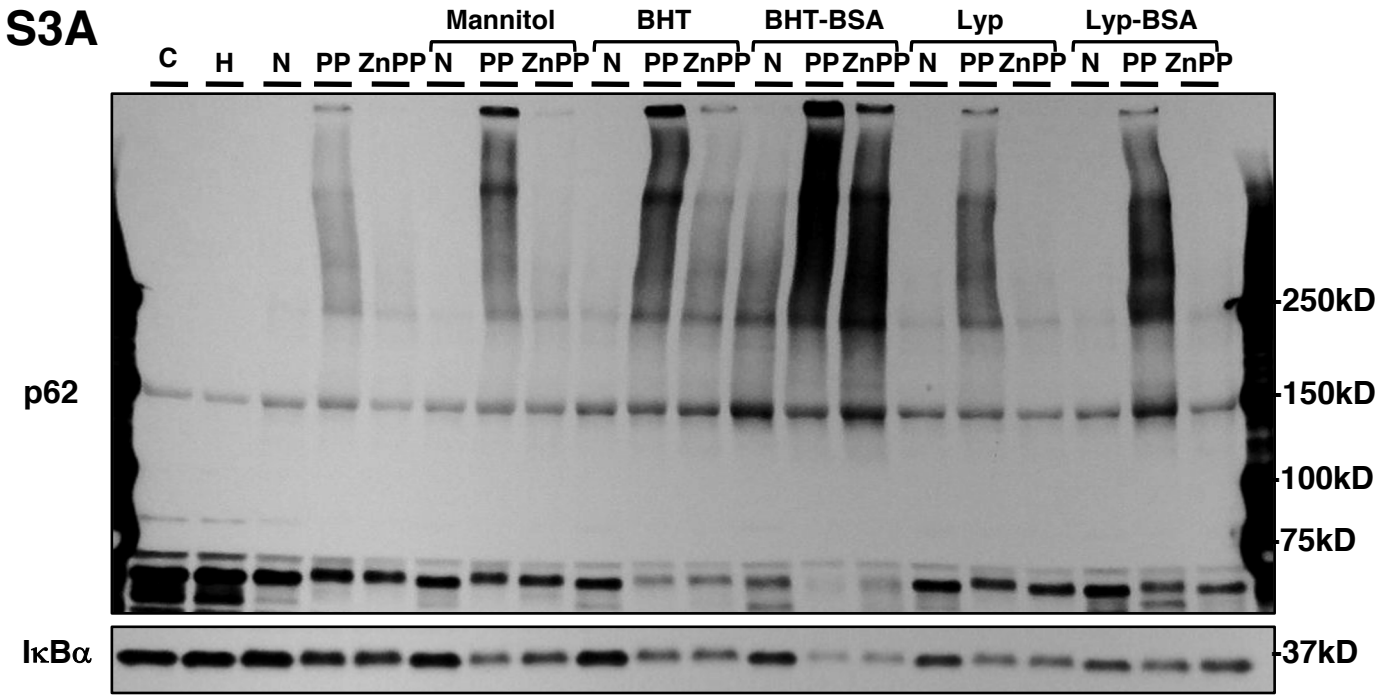

ROS Scavenger:
Mannitol: (soluble)
Hydroxyl radical (HO•)
BHT: (low solubility)
Peroxyl radical (ROO•)
Lycopene: (not soluble)
Singlet oxygen ($^1O_2$)

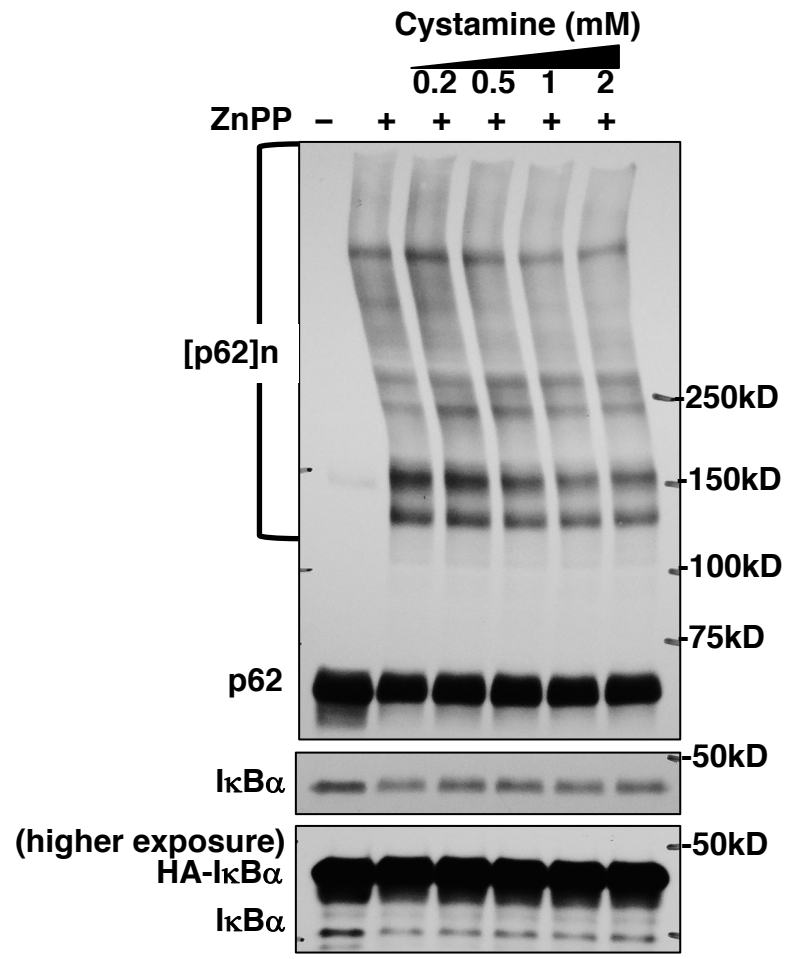

FIGURE S3. ZnPP-elicited IκBα-loss and p62 cannot be reversed by antioxidants or TG2 inhibitors (Related to Fig 1). **A**. Primary mouse hepatocytes were left untreated, or pretreated for 1 h with mannitol (50 mM), or BHT (100 μM), or lycopene (Lyp; 50 μM) , or BHT coupled with BSA to help keep it solubilized (BHT-BSA), or lycopene coupled with BSA (Lyp-BSA), and then treated with vehicle control (C), hemin (H; 10 μM), NMPP (N; 30 μM), or PPIX (PP; 10 μM), or ZnPP (10 μM) for 4 h as indicated. Cell lysates were used for IB analyses of p62 and IκBα. **B**. HEK293T cells were co-transfected with pcDNA6-p62-myc or pCMV4-3HA-IκBα. 48 h after transfection, cells were pretreated with various concentrations of cystamine as indicated and then treated with ZnPP (10 μM). for 2 h. Cell lysates were used for IB analyses of p62 and IκBα.

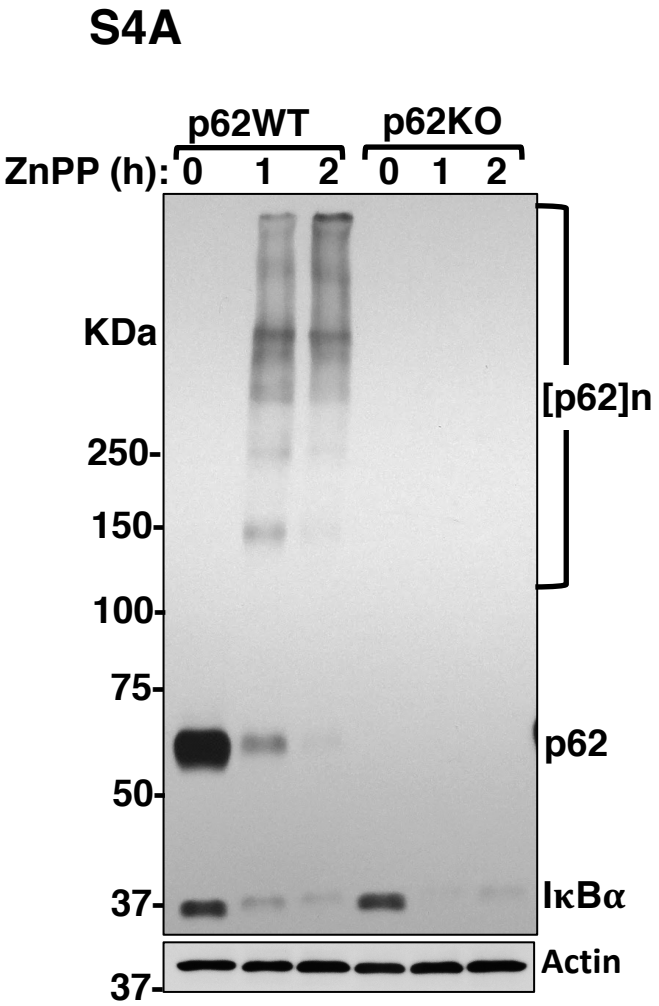

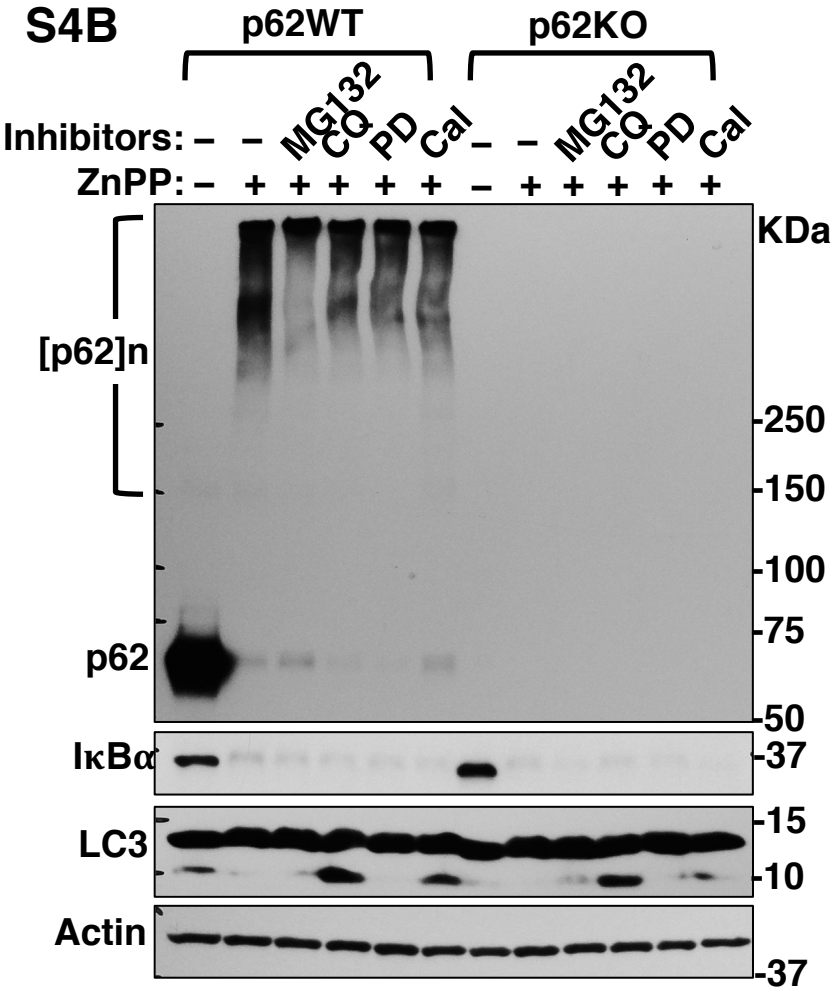

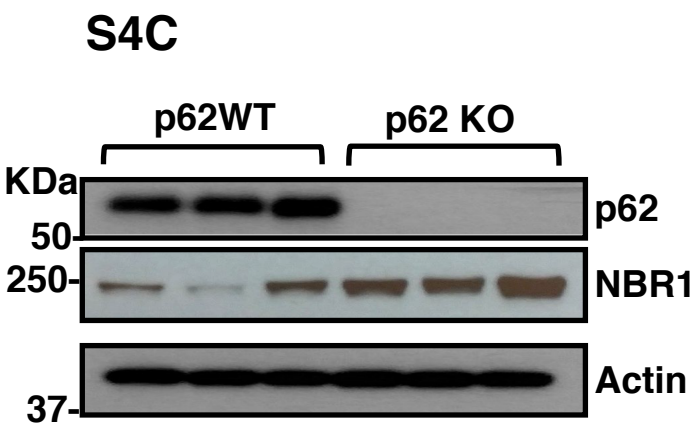

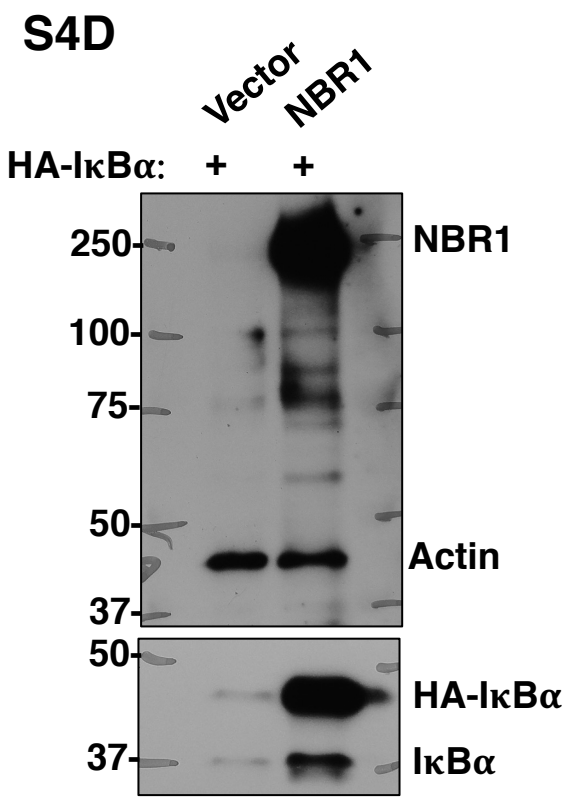

FIGURE S4. ZnPP-elicited IκBα-loss is independent of p62 and NBR1. (Related to Fig 2). **A.** p62WT and p62KO MEF cells were treated with 10 μM ZnPP for the indicated times. Cell lysates were used for IB analyses of p62 and IkBa, with actin as the loading control. **B.** p62WT and p62KO MEF cells were pretreated for 1 h with inhibitors of various protein degradation pathways: MG132 (20 μM; proteasomal), chloroquine (CQ, 100 μM; lysosomal), PD150606 (PD, 200 μM; calpain1/2), or calpeptin (Cal, 200 μM; cathepsin and calpain), and then treated with 10 μM ZnPP for 2 h. Cell lysates were used for IB analyses. **C**. Lysates from p62WT and p62KO primary mouse hepatocytes were used for IB analyses of p62, and NBR1 with actin as the loading control. The three lanes correspond to p62 WT and p62 KO hepatocytes from three individual mice. **D**. HEK293T cells were co-transfected with pCMV4-3HA-IκBα with either pcDNA3 empty vector or pcDNA3-NBR1 for 48 h. Cell lysates were used for IB analyses of NBR1 and IκBα with actin as the loading control.

S5A

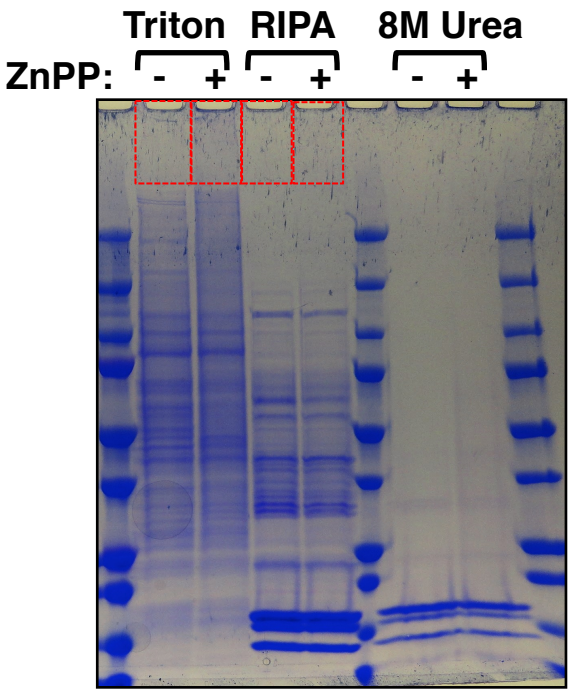

S5C

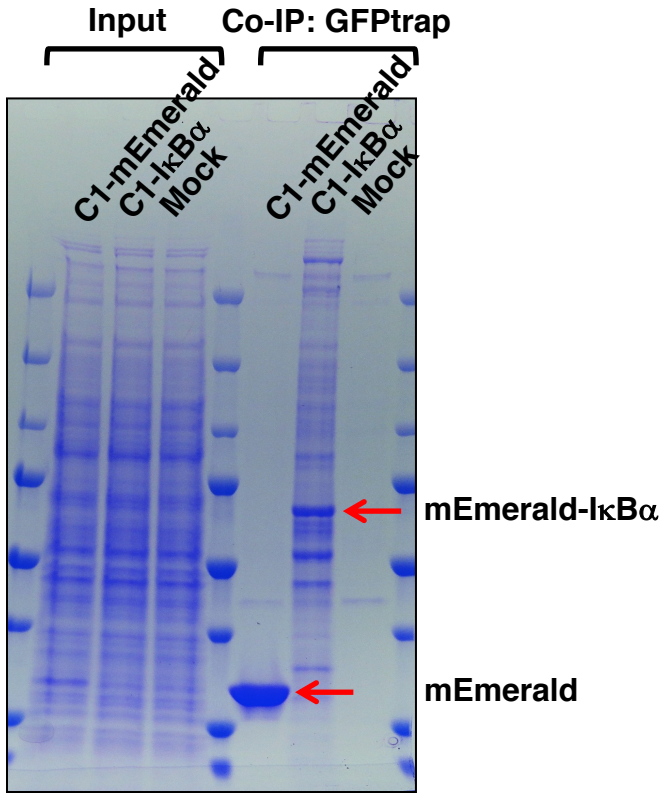

S5B

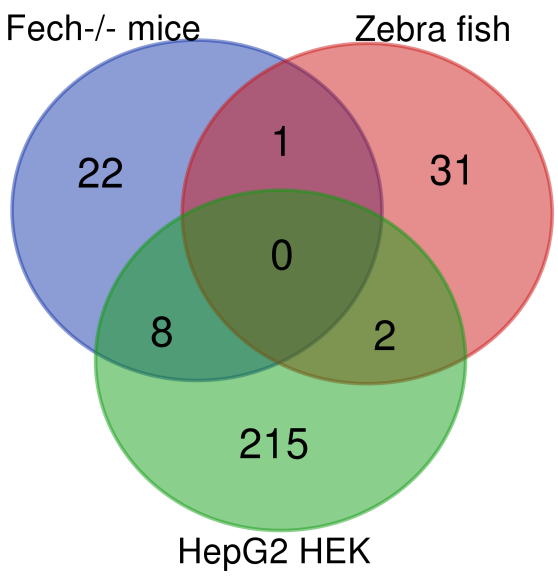

FIGURE S5. Representative gel images (Related to Fig 4, Fig 5). **A**. Representative Coomassie Blue staining of proteins from sequential Triton, RIPA and urea fractions. HMM-fractions of Triton and RIPA extracts (demarcated by the red boxes) were excised from the gel for in-gel digestion and the entire urea fraction were used for in-solution digestion followed by MS analyses (LC-MS/MS) **B**. Venn Diagram of 225 HepG2/HEK293T common ZnPP-induced aggregate proteins with aggregate proteins form Fech$^{-/-}$ mouse model (8,13,59) and protoporphyric zebra fish model (60). **C**. Representative Coomassie Blue staining of lysates before and after immunoaffinity purification (IAP).

S6A

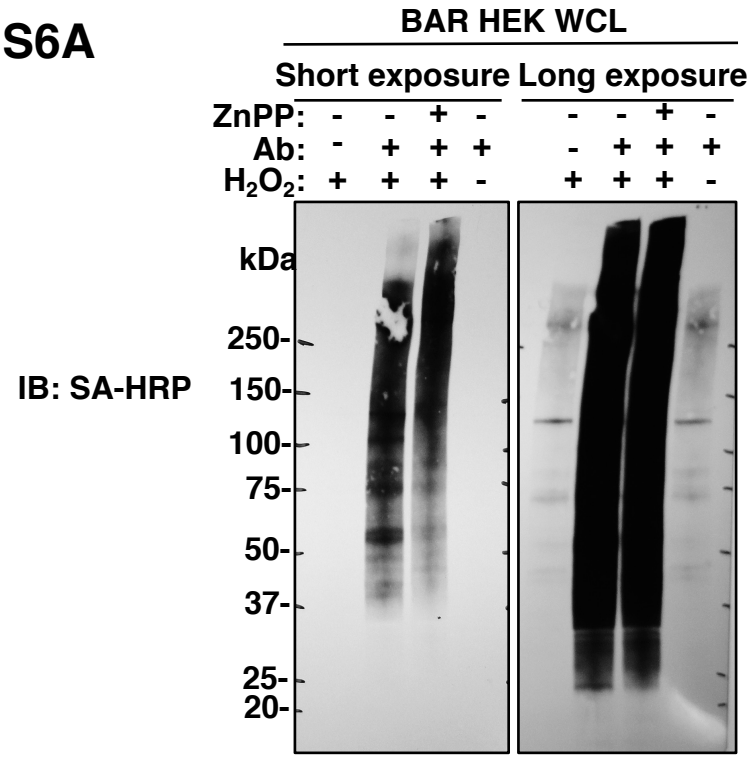

S6B

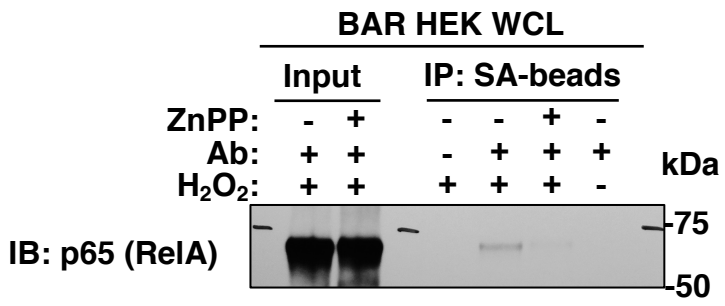

S6C

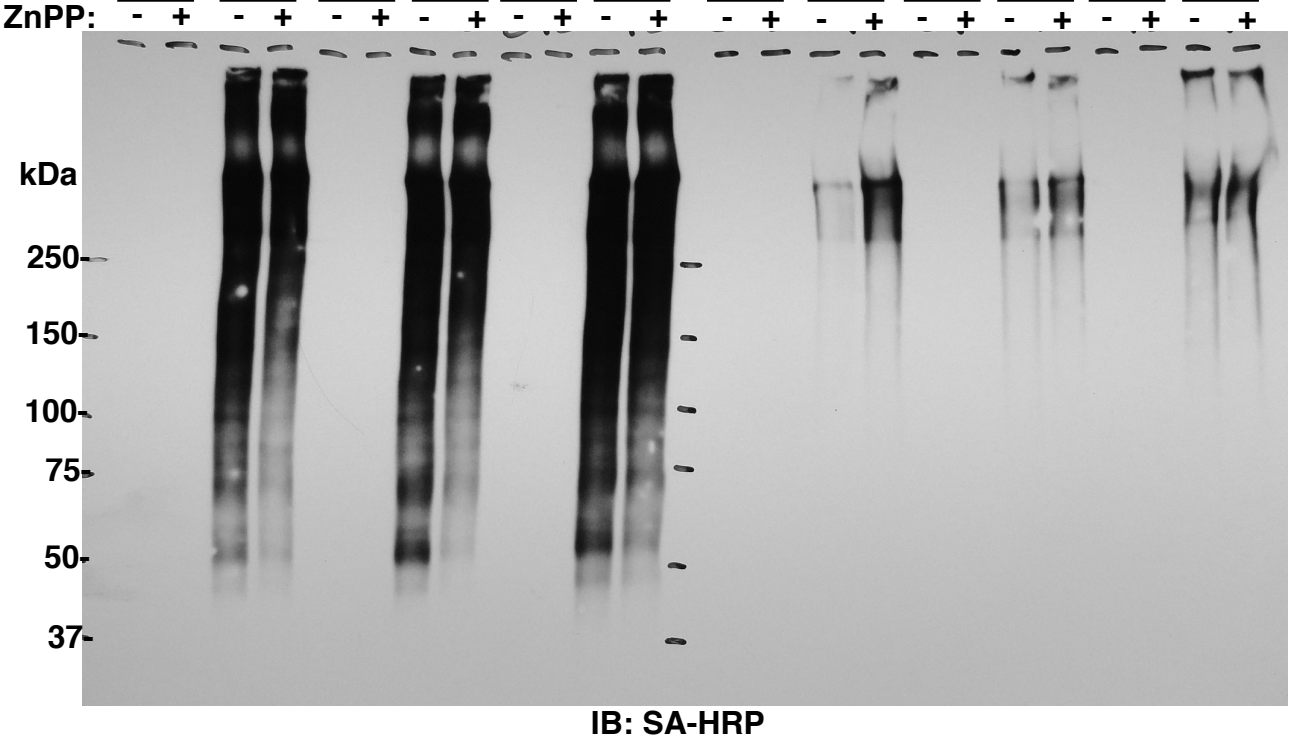

S6D

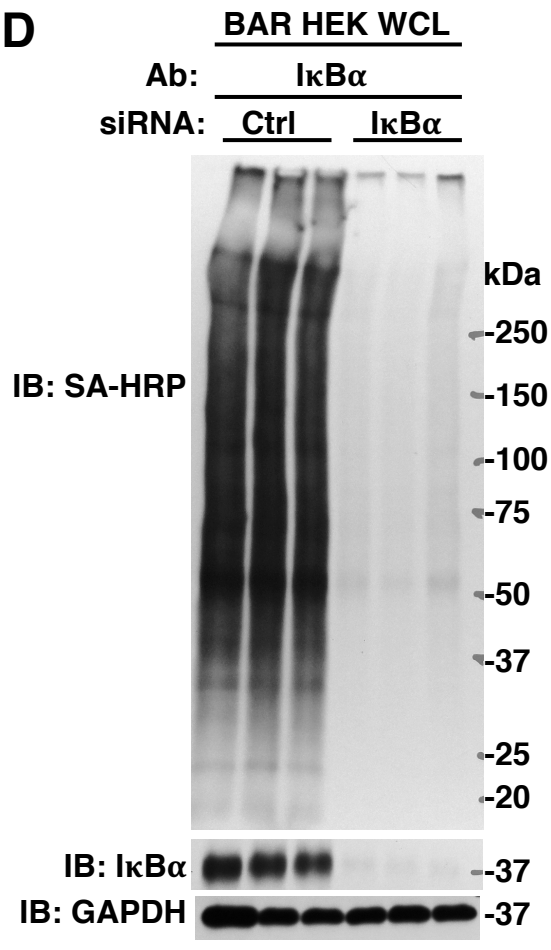

S6E

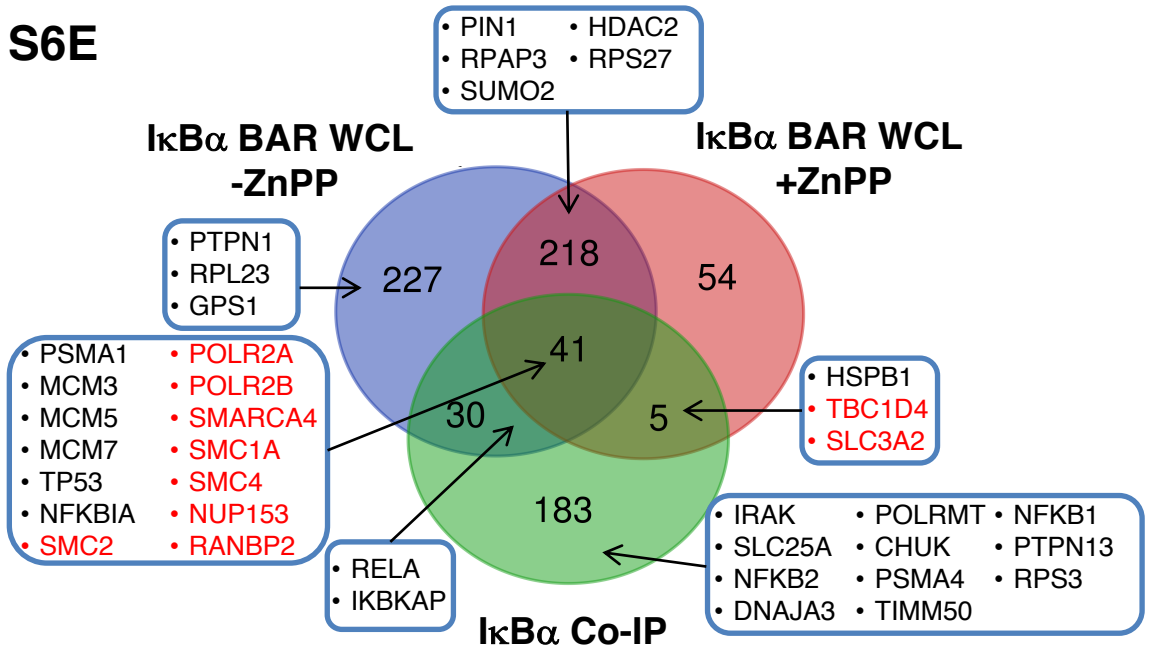

FIGURE S6. Characterization of biotinylation via IκBα-antibody recognition (BAR). (Related to Fig 5B). **A.** HEK293T cells were transfected with with pCMV4-3HA-IκBα for 48 h. Some cells were treated with ZnPP (10 μM) for 2 h. Cells were fixed and then stained with IκBα-antibody for downstream HRP-antibody recognition dependent biotinylation labeling (BAR) as described in Methods. Cells were lysed, sub-fractionated into whole cell lysates (WCL) and pellet as described in Methods, separated by SDS-PAGE and analyzed by blotting with streptavidin-HRP. Negative controls in which IκBα-antibody or H_2O_2 was omitted are shown in lanes 1 and 4 of each blot. The band pattern shows that biotinylation is dependent on the presence of both IκBα-antibody and H_2O_2, suggesting the specificity of biotinylation of endogenous IκBα-proximal proteins. The up-shift of bands in WCL fraction and an increased intensity of bands in the pellet fraction in ZnPP-treated cells suggest that IκBα interacts with ZnPP-aggregated proteins. After higher exposure, in the negative control lanes from WCL fraction, some faint bands representing endogenous biotinylated proteins are detected (i.e. 130, 75 and 72 kDa). **B**. Biotinylated proteins from (**A**) were enriched using streptavidin-coated magnetic beads, separated by SDS-PAGE and analyzed by blotting with p65 antibody (a known IκBα-interactor). The disappearance of p65 in the negative controls without IκBα-antibody and without H_2O_2 suggest the specificity of BAR analyses. The disappearance of p65 in ZnPP-treated samples after BAR suggests p65 no longer binds to IκBα after ZnPP-treatment. **C**. BAR experiments were repeated as described in (**A**), but with the modified negative controls, IgG-staining as control for IκBα-staining, and IgG-staining after ZnPP-treatment as a negative control for IκBα-staining after ZnPP-treatment. Both whole cell lysates (WCL) and pellet fractions were analyzed by blotting with streptavidin-HRP. **D**. HEK293T cells were transfected with control non-targeting siRNA or IκBα-siRNA for 48 h, followed by fixation and IκBα BAR as described in Methods. 10 ug WCL were analyzed by blotting with streptavidin-HRP, IκBα-antibody and GAPDH-antibody. **E**. Biotinylated proteins from (**C**) WCL fractions and (**D**) were enriched using streptavidin-coated magnetic beads and trypsin/Lys-C digested for LC-MS/MS proteomic analyses. Specific IκBα-interactors with and without ZnPP treatment were identified by analyzing LC-MS/MS data with SAINTexpress, using IgG-staining and IκBα-staining in IκBα knockout cells as negative controls. The numbers of proteins identified using BAR WCL in cells treated with or without ZnPP in comparison with the co-IP method are shown in the Venn diagrams, with known IκBα-interactors from the iRefIndex listed in black. 10 novel IκBα-interacting and -aggregating proteins identified in Fig 5D are also listed in red.

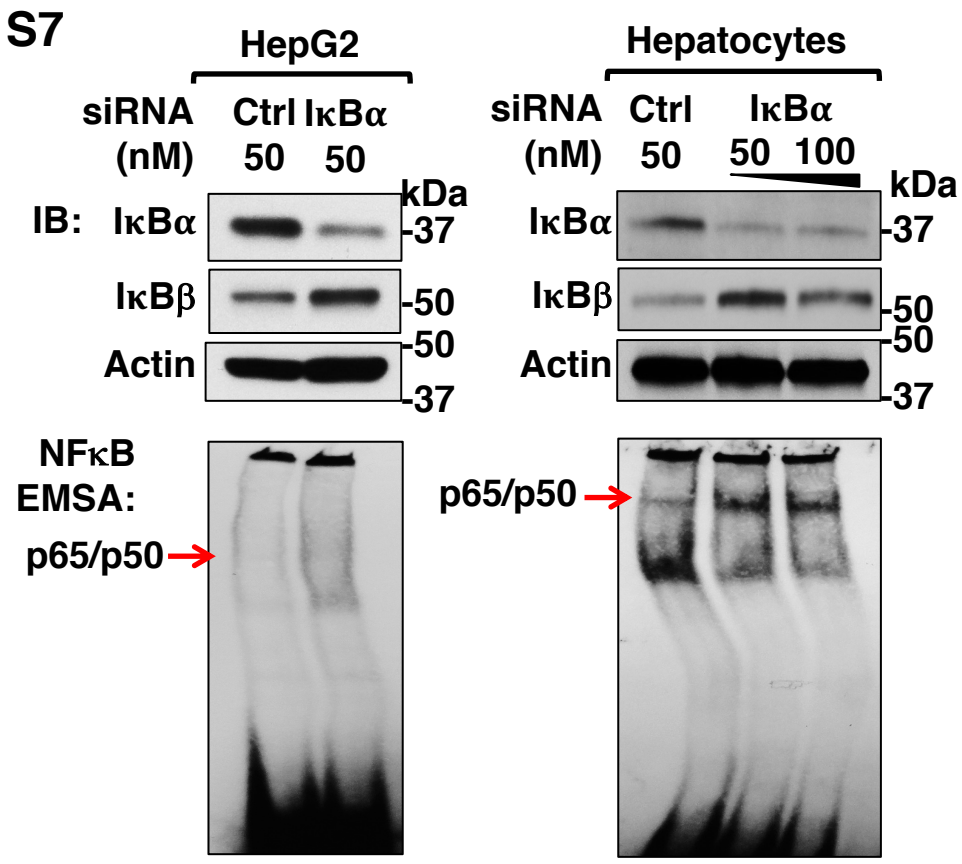

FIGURE S7. **(Related to Fig 8)** Effects of of IκBα siRNA knockdown on IκBβ-levels and constitutive NF-κB-activation. siRNA knockdown and EMSA analyses were conducted as detailed in Experimental procedures.